Experimental and Theoretical Performance Assessment of WiFi-over-Fiber Using Low Cost Directly Modulated VCSELs

D. Coelho[1,2], J. M. B. OLiveira[1,2], L. M. Pessoa[1], J. C. S. Castro[1], H. M. Salgado[1,2]
[1]INESC TEC
[2]Faculty of Engineering, University of Porto,
Porto, Portugal
Tel: (351) 222 094 000, Fax: (351) 222 094 050
e-mail: {dcoelho, joao.b.oliveira, luis.m.pessoa, henrique.salgado, jorge.castro}@inescporto.pt

ABSTRACT

In this work, an in-depth analysis concerning the transmission performance of IEEE802.11g/n WiFi signals in a radio-over-fiber system is presented. Low-cost optical/electrical transceivers based on 850 nm vertical cavity surface emitting lasers (VCSELs) and PIN photodiodes are considered. System modelling includes the impact of noise generated in the optical path, such as relative intensity noise (RIN), shot noise, photodetector thermal noise, clipping and intermodulation distortion. Analytic results based on Volterra series analysis for the performance of the system in terms of SNR and EVM for several optical modulation index values are obtained. The theoretical analysis is also compared with experimental results. Among several conclusions, it is observed that the laser intermodulation distortion, clipping and RIN are the most relevant factors

Keywords: WiFi, Radio-over-Fiber, VCSELs, intermodulation distortion, signal-to-noise ratio, error vector magnitude.

1. INTRODUCTION

RoF systems can be completely transparent to all signals conveyed in the optical channel. It has been experimentally demonstrated that RoF networks are well suited to simultaneously transport several wireless standards like wideband code division multiple access (WCDMA), IEEE 802.11 wireless local area network (WiFi) [1], global system for mobile communications (GSM) [2], WiMAX [3] and ultra-wide band (UWB) [4].

The RF signals transmitted through the optical link can suffer several impairments such as intermodulation distortion, relative intensity noise (RIN), shot noise, photodetector thermal noise and clipping.

Due to the large number of electrical subcarriers of the WiFi signal, a high nonlinear distortion may be expected from the electrical to optical conversion when using directly modulated laser diodes, such as VCSELs. The most troublesome intermodulation distortion products (IMPs) are the third-order ones since they lie within the transmission band. The maximum fiber length of the optical network is considered to be 100 meters. Thus, it is reasonable to neglect both the attenuation and dispersion of RF signals with frequencies up to 10 GHz [5].

In this paper, the impairments generated in a point-to-point RoF link modulated by a VCSEL are analysed. The work is divided in four sections. Section 2 describes the theoretical analysis of the RoF system architecture. Section 3 presents the results obtained considering all noise contributions and nonlinear impairments. Finally, section 4 highlights the main conclusions.

2. PERFORMANCE ASSESSMENT ANALYSIS

Let us consider the point-to-point architecture shown in the Fig.1.

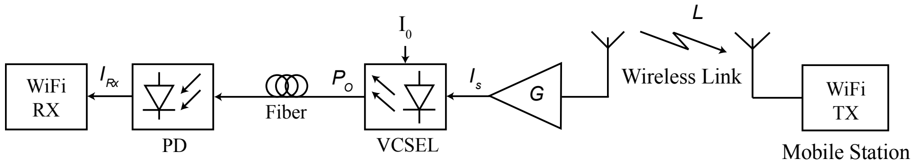

Figure 1. Point-to-point transmission scheme.

The RF uplink signal is generated by the Mobile Station and reaches the base station attenuated by the wireless channel. The weak RF uplink signal is then electrically amplified (*G*) before being converted from the electrical to the optical domain by the VCSEL. In the central station, the optical signal is detected by a PIN photodetector which converts the optical signal to the electrical before reaching the WiFi receiver module (WiFi Rx). The RF signal detected will suffer the impact of the RIN noise, shot noise, photodetector thermal noise, clipping and intermodulation distortion.

The SNR for the uplink path, referred at the output of the photodiode optical receiver, can be written as [6],

$$SNR_{up} = \frac{\langle I_{Rx}^2 \rangle}{\langle I_{RIN}^2 \rangle + \langle I_{SN}^2 \rangle + \langle I_{th}^2 \rangle + \langle I_{dist}^2 \rangle + \langle I_{clip}^2 \rangle} \qquad (1)$$

where the five current noise terms are: the RIN noise current, the shot noise current, the thermal noise current from the equivalent resistance of the photodetector (PD) load and amplifier (R_{eq}), the current due to the third order intermodulation distortions and the current due clipping distortions, respectively. The source thermal noise can be neglected and $\langle I_{Rx}^2 \rangle$ is the signal power at the receiver [6]-[7].

$$\langle I_{Rx}^2 \rangle = \frac{1}{2}\left(r_d\, \mu \sqrt{\frac{2}{N}} \langle P_o \rangle \right)^2 \qquad (2)$$

$$\langle I_{RIN}^2 \rangle = r_d^2 \langle P_o^2 \rangle 10^{\frac{RIN}{10}} \Delta f \qquad (3)$$

$$\langle I_{SN}^2 \rangle = 2qr_d \langle P_o \rangle \Delta f \qquad (4)$$

$$\langle I_{th}^2 \rangle = {4kTF\Delta f}/{R_{eq}} \qquad (5)$$

$$\langle I_{dist}^2 \rangle = \frac{1}{2}\left(r_d \langle P_o \rangle \right)^2 \left(\mu \sqrt{\frac{2}{N}} \right)^6 (D_{111}N^2 + D_{21}N) \qquad (6)$$

$$\langle I_{clip}^2 \rangle = \frac{1}{\sqrt{2\pi}} \Lambda r_d \langle P_o \rangle \frac{\mu^5}{1+6\mu^2} e^{\frac{-1}{2}\mu^2} \qquad (7)$$

Each of the noise terms are given in equations (2)-(7), where the r_d parameter is the photodetector responsivity, P_o is the average optical power detected by the PD, I_0 is the average photocurrent detected, Δf is the electrical bandwidth of the receiver, q is the electronic charge, k is Boltzmann's constant, T=290 K, F is the noise factor of the amplifier following the PD and D_{111} and D_{21} are the third-order distortion coefficients, corresponding to IMPs of type $f_i + f_j - f_k$ and $2f_i - f_j$, respectively. These depend on the laser characteristics and operation point. The μ parameter is the total rms modulation index and is equal to $\mu = m\sqrt{N/2}$, where m is the optical modulation index per subcarrier. The Λ parameter represents the fraction of the clipping distortion power which falls in the transmission band which is also dependent on the optical modulation index [8]. For the specific channel allocation, $\Lambda = 1.1\times10^{-3}$ for μ=2%.

Volterra functional series, described as a "power series with memory", has been applied previously to assess accurately the laser distortion of the semiconductor laser [9]. The latter analysis enables one to determine adequately the third-order intermodulation coefficients of the semiconductor laser, considering the allocation of subcarriers for WiFi (2.4 GHz-2.42 GHz). Table 1 presents the intrinsic laser parameters of the FINISAIR HFE-4192-582 VCSEL operating at 850 nm, which have been extracted using the frequency subtraction method [10].

Table 1. Intrinsic parameters of FINISAIR HFE-4192-582.

Parameter	Symbol	Value	Unit
Volume of the active region	V	2.4×10^{-18}	m^3
Gain slope constant	g_o	4.2×10^{-12}	m^3s^{-1}
Compression factor	ε	2.0×10^{-23}	m^3
Electron density at transparency	N_{0m}	1.9×10^{24}	m^{-3}
Spontaneous emission factor	β	1.7×10^{-4}	—
Optical confinement factor	Γ	4.5×10^{-2}	—
Photon lifetime	τ_p	1.8	ns
Carrier lifetime	τ_n	2.6	ps
Injection efficiency	η_i	0.8	

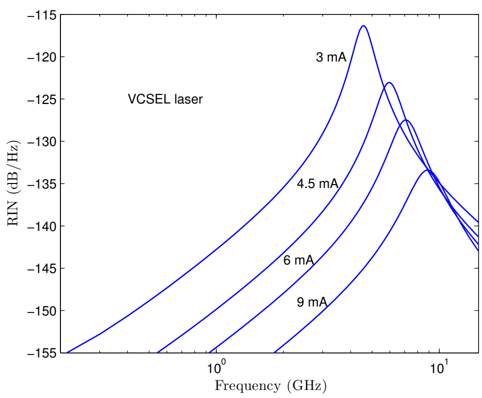

Figure 2. Relative Intensity Noise of the laser.

The bias current I_{th} = 1.4 mA and the slope efficiency of this laser is 0.059 A/W. The relative noise intensity characteristic of this VCSEL, obtained from the rate equation with Langevin noise sources is represented in Fig. 2. In the range of 3 to 9 mA RIN varies between -152 to -133 dB/Hz. Fig. 3 and Fig. 4 shows the distortion coefficients (D_{111} and D_{21}) for each subcarrier transmission for several values of bias current applied to the VCSEL.

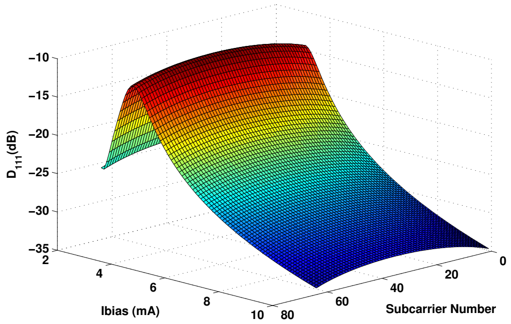

Figure 3. D_{111} for several bias current

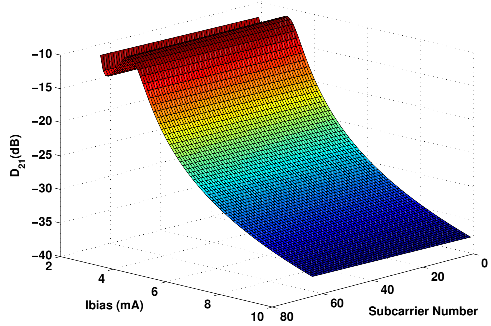

Figure 4. D_{21} for several bias current

The D_{111} coefficient has the major impact in the IMD limitation since it increases with N^2, while the D_{21} contribution increases with N (eq. (6)). Also from Fig. 3 and Fig. 4, it is seen that a better performance is expected when the VCSEL is operated at 9 mA of bias current and a worst performance at 3 mA, when considering the IMD impact on the system performance. For a bias current of 3 and 5 mA, D_{111} is maximum for the subcarrier number 34 and 35, and equals 0.0522 and 0.0057, respectively. The corresponding maximum values for D_{21} occur for subcarrier number 63 and 64, and are 0.0081 and 0.0034, respectively. The resonance of the laser may actually change the location within the band (subcarrier) where we would expect the maximum distortion to occur (middle channel for D_{111} and last channel for D_{21}).

3. THEORETICAL AND EXPERIMENTAL RESULTS

In this section the previous theoretical analysis, based on SNR, is compared with experimental results. Experimentally the performance of the system is assessed in terms of error vector magnitude (EVM), which relates to the SNR by $EVM = 1/\sqrt{SNR}$ [11]. The experimental setup used is depicted in Fig. 5. It is composed of a vector signal generator (R&S SMJ 100A) to generate the WiFi signal, an electrical to optical converter (VCSEL model FINISAIR HFE-4192-582), an optical to electrical converter (81495A) and a Digital Serial Analyzer (Tektronics DSA 71254C) for the signal analysis and EVM measurements.

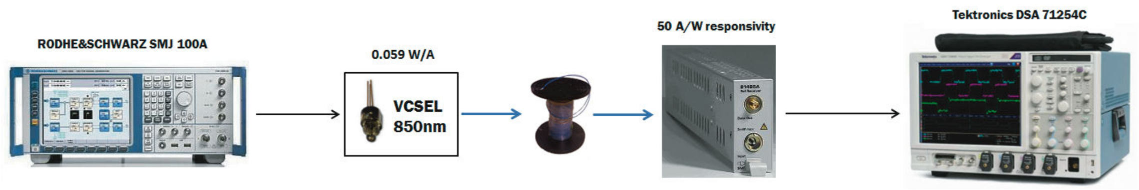

Figure 5. Diagram of experimental setup.

Fig. 6-a) and b) show the results of both analytical and experimental SNR as a function of the total rms modulation index, for the uplink point-to-point transmission scheme. The noise limiting contributions are plotted in the graph as well. A minimum SNR of 20 dB can be specified considering a typical sensitivity from a commercial IEEE 802.11n of -74 dBm, in the 2.4 GHz band [12].

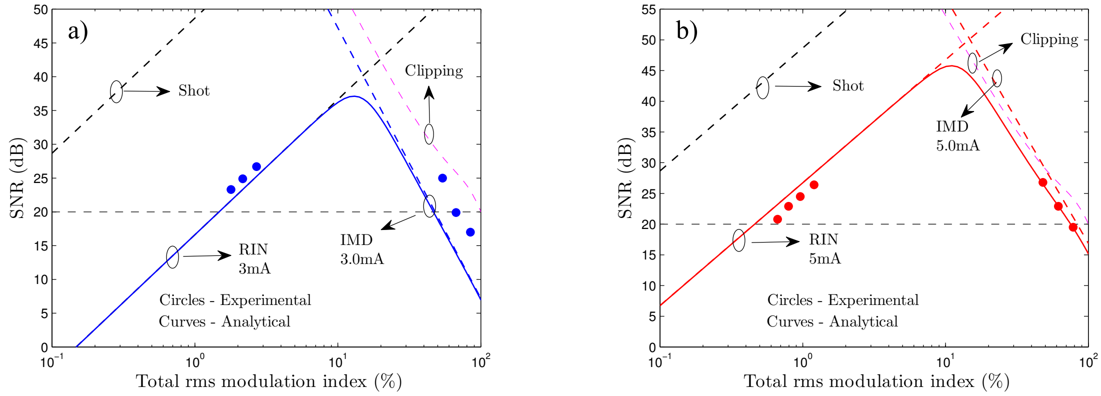

Figure 6. Analytical and experimental results: a) I_{bias}=3 mA; b) I_{bias}= 5 mA.

From the results we can see that the best performance in terms of SNR is achieved at high bias currents, when the intermodulation distortion is lower and the performance is limited by both clipping and IMD. The maximum SNR value for a bias current of 3 mA is 37.12 dB for a total rms modulation index of 13%, while for a bias current of 5 mA, the maximum SNR is 45.78 dB for a total rms modulation index of 11%.

The experimental results confirm the predicted behavior in the region where RIN and distortion are dominant, showing good agreement with the theoretical results. Experimentally it was not possible to reach the maximum SNR, since the EVM values reached a plateau that we are unable to explain.

4. CONCLUSIONS

In this article, we have considered the transmission of WiFi signals through an optical channel. In particular, we analyze the uplink performance in a point-to-point transmission system for short range networks.

A theoretical analysis was performed and a good agreement with the experimental results was obtained.

Both analytical and experimental results show that, for low bias currents, the intermodulation distortion is the main limiting performance factor at high modulation indexes, whereas the RIN is the dominant factor for low modulation indexes. For increasing bias current, the IMD distortion decreases and clipping distortion starts to dominate over intermodulation distortion, at high modulation indexes. The detailed analysis presented is adequate for the performance assessment and design of radio-over-fiber systems.

ACKNOWLEDGEMENTS

We acknowledge funding from FCT and program POCTI/FEDER under the National Plan for Scientific Hardware Renewal with grant EEQ/1272/EEI/2005. D. Coelho also acknowledges support from FCT through a PhD grant. This work was supported in part by EC Framework 7 (FP7) project DAPHNE (www.fp7daphne.eu) – Developing aircraft photonic networks (grant ACP8-GA-2009-233709).

REFERENCES

[1] J.E. Mitchell: Performance of OFDM at 5.8 GHz using radio over fibre link, Electronics Letters, vol.40, no.21, pp. 1353-1354, 14 October, 2004.

[2] P.K. Tang, L.C. Ong, A. Alphones, B. Luo, M. Fujise: PER and EVM measurements of a radio-over-fibre network for cellular and WLAN system applications, Journal of Lightwave Technology, vol. 22, no. 11, pp. 2370–2376, November, 2004.

[3] N.J. Gomes, M. Morant, A. Alphones, B. Cabon, J.E. Mitchell, C. Lethien, M. Csörnyei, A. Stöhr, S. Iezekiel: Radio-over-fibre transport for the support of wireless broadband services, Journal of Optical Networking, vol. 8, no. 2, pp. 156-178, Feb., 2009.

[4] M. Jazayerifar, B. Cabon, J.A. Salehi: Transmission of multi-band OFDM and impulse radio ultra-wideband signals over single mode fibre, Journal of Lightwave Technology, vol. 26, no. 15, pp. 2594–2603, Aug. 1, 2008.

[5] C.H. Cox III, E.I. Ackerman, G.E. Betts, L.P. Prince: Limits on the Performance of RF-Over-Fiber Links and Their Impact on Device Design, IEEE Transactions on Microwave Theory and Techniques, vol. 54, nº 2, February 2006.

[6] C.H. Cox III: Analog Optical Links: Theory and Practice. Cambridge: Cambridge University Press, 2004.

[7] A. A. M. Saleh: Fundamental limit on number of channels in subcarrier multiplexed lightwave CATV system, Electron. Lett., vol. 25, pp. 776–777, June 1989.

[8] J. E. Mazo: Asymptotic distortion of clipped, dc-biased, gaussian noise, *IEEE Trans. Commun.,* vol. 40, no. 8, pp. 1339-1344, Aug. 1992.

[9] H. M. Salgado and J. J. O'Reilly, Volterra series of distortion in semiconductor lasers, IEE Proceedings-J Optoelectronics, vol. 138, no. 6, 1991.

[10] P.A Morton, et. Al: Frequency response subtraction for simple measurement of intrinsic laser dynamic properties, IEEE Photon Technol. Lett., vol.4, pp.133-136, Feb. 1992.

[11] K. Ghairabeh, K. Gard, and M. Steer: Accurate Estimation of Digital Communication System Metrices - SNR, EVM and ρ in a Nonlinear Amplifier Environment, IEEE Transactions on Communications, pages pp.734–739, September 2005.

[12] W. N. Corporation: Product Specifications of DNMA-92, An IEEE 802.11n a/b/g/n Mini-PCI module, version 1.6, April 2009.